




## Article

# Ecological and Human Health Risk Assessment Based on Stream Sediments from Coastal Oecusse (Timor)

Victor A. S. Vicente <sup>1</sup>, Marina Cabral Pinto <sup>2,\*</sup>, Pedro Dinis <sup>3</sup> and João A. M. S. Pratas <sup>1,4</sup>

<sup>1</sup> Instituto de Geociências de Timor-Leste (IGTL), City 8, CBD Level 2, Rua Has-Laran, Manleuana, Dili, Timor-Leste; victor.vicente@igt.tl (V.A.S.V.); joao.pratas@igt.tl (J.A.M.S.P.)

<sup>2</sup> GeoBioTec Centre, Department of Geosciences, Campus de Santiago, University of Aveiro, 3810-193 Aveiro, Portugal

<sup>3</sup> MARE—Marine and Environmental Sciences Centre, ARNET—Aquatic Research Network, Department of Earth Sciences, Rua Sílvio Lima—Polo II, University of Coimbra, 3030-790 Coimbra, Portugal; pdinis@dct.uc.pt

<sup>4</sup> Centro de Geociências da Universidade de Coimbra, Universidade de Coimbra-Polo II, 3030-790 Coimbra, Portugal

\* Correspondence: marinacp@ua.pt

**Abstract:** Timor Island is located in a geologically complex region strongly affected by the collision of the Australian margin with the Banda volcanic arc. In Oecusse, an enclave of East Timor in the western part of Timor, crop out several lithological units of the Banda Terrane that are associated with the obduction of oceanic crust and upper mantle on the Australian continental crust. This study reports the geochemistry of stream sediments from the coastal region of the Oecusse enclave, where the Banda Terrane is best represented, employing statistical analyses to discern the sources of metal(oid)s and assessing ecological and health risks. Arsenic, Cr, and Ni are the elements with higher potential ecological risk factors. The potential ecological risk index (PERI), which combines single indexes of ecological risk factors for multiple elements, is very high in a stream sourced by the Lolotoi-Mutis Complex. Significant risks for human health were found for As (sourced by the Lolotoi-Multis Metamorphic Complex and basalts of the Barique Formation), Mn (sourced by the Maubisse and Barique formations), and V (sourced by the Manamas Formation). The highest values of hazard index (HI), however, were determined with Cr, in particular for children (HI higher than 10 in 12 sediments sourced by ultramafic units and their covering sedimentary units). This investigation shows that high geogenic concentrations of several elements, particularly those derived from the oceanic crust and the upper mantle, raise significant cancer and non-carcinogenic risks.

**Keywords:** geochemistry; potential ecological risk index; human health risks; arc-continent collision; Oecusse



**Citation:** Vicente, V.A.S.; Cabral Pinto, M.; Dinis, P.; Pratas, J.A.M.S. Ecological and Human Health Risk Assessment Based on Stream Sediments from Coastal Oecusse (Timor). *Water* **2024**, *16*, 3020. <https://doi.org/10.3390/w16213020>

Academic Editor: Achim A. Beylich

Received: 27 August 2024

Revised: 24 September 2024

Accepted: 15 October 2024

Published: 22 October 2024



**Copyright:** © 2024 by the authors. Licensee MDPI, Basel, Switzerland. This article is an open access article distributed under the terms and conditions of the Creative Commons Attribution (CC BY) license (<https://creativecommons.org/licenses/by/4.0/>).

## 1. Introduction

The planetary health manifesto goal is to create a movement for planetary health, a planet that nourishes and sustains the diversity of life with which we coexist and on which we depend [1]. It is a social movement to support collective public health action at all levels of society—personal, community, national, regional, global, and planetary [1]. The main objective is to protect against threats to human health and well-being, threats to the sustainability of our civilization, and threats to the natural and human-made systems that support us. Within planetary health, it is essential to characterize the linkages between environmental changes and human health at different geospatial and temporal scales. Since the last century, our planet developed into a changed new phase, and life, as we have known it for the last ten times, is altering very fast [2]. As natural systems undergo unprecedented modifications, both our well-being and the health of the planet are at risk [2,3]. Humans are part of nature, and its health cannot be separated from the health of the environment [3–5].

Given the present environmental conditions, geochemical mapping has become an urgent priority in many countries. This urgency is evident across various scales due to the significant importance and wide-ranging applications of the geochemical data collected (e.g., [6–15]). Stream sediments frequently offer a composite sample from the upstream catchment area [16,17]. This medium effectively integrates all sources of sediment, including primary rock and soil, and serves as a reliable representation of the geochemical background [16–18]. Changes in the chemical composition of natural media, such as sediments, dust, soils, and ground and surface waters, might induce metabolic changes leading to the occurrence of endemic diseases and ecological risks (e.g., [19–21]). Nowadays, there has been more focus on the neurotoxic and also potential carcinogenic effects of environmental and occupational exposure to metal (loid)s, such as Al, As, Cd, Co, Cr, Cu, Mn, Ni, Pb, and Zn [22–56]. For instance, the International Agency for Research on Cancer has identified occupational exposure to chromium [VI] and nickel compounds as carcinogenic to humans [57], exposure to cadmium and lead is linked to changes in kidney function [53–56], cadmium and chromium are linked to hypertension and atherosclerosis [53,54], and there seems to be a connection between the inhalation and ingestion of manganese and complaints of the central nervous system in humans [58–61].

Stream sediments capture the geochemical properties of their source materials. They can become naturally contaminated as rocks containing potentially toxic elements (PTEs) undergo weathering. This natural contamination can have implications for both ecological health and human well-being [16,17,62–64]. The impact of eventual contamination is not confined to the area near the source, as contaminated materials can be physically transported, especially during periods of high runoff. This can result in the spread of pollutants over great distances, potentially harming plants, animals, and humans far from the original source [65]. Studying the geochemistry of the near-surface environment, including the interactions between rocks, soil, sediments, and water, provides a valuable tool for assessing potential natural risks to ecological and human health. This includes the risk of endemic diseases that may result from prolonged or elevated exposure to these geochemical elements. Such risks can be subtle, long-lasting, and sometimes irreversible [66–68].

Since 2016, the Institute of Geosciences of East Timor (former Institute of Petroleum and Geology) has performed in the Oecusse enclave, in the western part of Timor Island, detailed geological recognition including stream sediment sampling. Sampled sediments were investigated to establish the geochemical baseline conditions and possible mineral resources [69]. These surveys revealed high contents of Cr, Ni, and Co in stream sediments sourced by ultramafic complexes that were not known in the region until then. Also, in Oecusse, high grades of Au and Cu were already reported [70,71]. A recent study focused on Indonesia [61,72] found high contents of Pb and Cr in surface water, with possible negative impacts on public health.

Chronic exposure to the metal(loid) reported as abundant in the study region (Cr, Ni, Co, Cu, Pb, As, Mn) can lead to negative effects on both human health and ecosystems [73–86]. This study aims to (i) identify the sources of metal(oid)s by integrating geochemical data with geological mapping and (ii) assess the ecological risk and health risk for children and adults.

## 2. Natural Setting

The island of Timor is located in Southeast Asia, approximately 700 km northwest of Darwin, Australia. Timor is part of the Outer Non-Volcanic Banda Arc that is genetically linked with the collision between the Volcanic Banda Arc and the Australian continental margin [87–89]. The arc-continent collision has produced a complex geological structure comprising juxtaposed units with Australian and Asian affinity, synorogenic sedimentary deposits, and a *mélange*.

The research area is located in the northern part of the Oecusse enclave (Figure 1), which is surrounded by the Nusa Tenggara Timur Province (NTT), Indonesia, and bordered by the Savu Sea to the north. In this region crop out 3 major tectonostratigraphy units [87–89]: (1) Gondwana Megasequence, with Permian to Middle Jurassic formations

deposited in the margin of Gondwanaland portion presently belonging to Australia; (2) Banda Terrane, dominated by Jurassic to Miocene rock formations with Asian affinity, including a metamorphic Complex, associated with high-degree metamorphisms, and covering siliciclastic successions, shallow marine limestones and outer neritic mudstones; (3) Synorogenic Megasequence, composed of Late Miocene to Pleistocene rock formations. This tectonostratigraphic unit covers a diapiric mélange, also known as Bobonaro Mélange, with rock blocks recognizably derived from most stratigraphic units on Timor enfolded in a mud matrix.

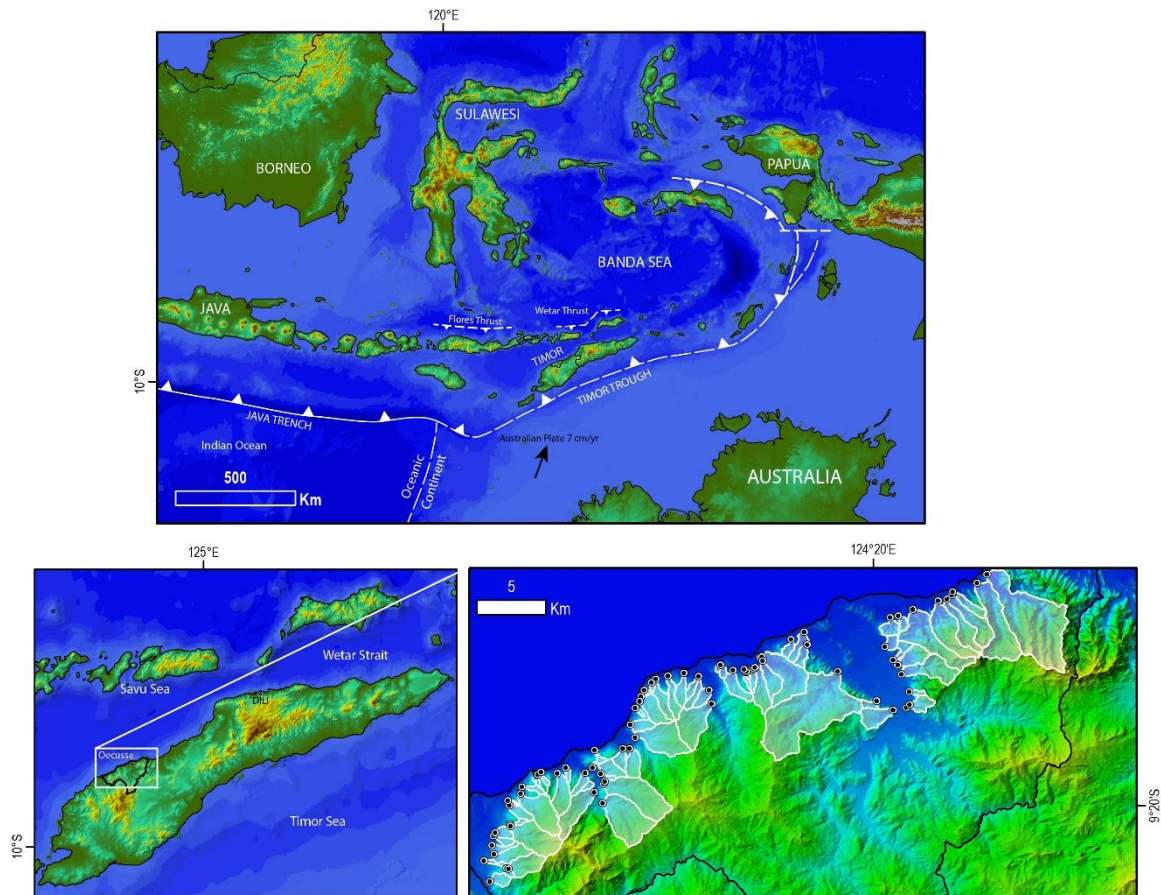


**Figure 1.** The location of the research area, Timor Island between Australia and the Banda Arc, and the drainage basins for the sampled stream deposits used in the present investigation.

The Gondwana Megasequence, with Australian affinity (Figure 2), comprises (1) Permian Maubisse Formation, with pillow basalts and well-bedded limestones; (2) Interbedded calcative-shale of Triassic Aituto Formation; (3) Triassic Babulu Formation with mudstones and turbiditic sandstones. The Aileu Complex, with mica schist, calcsilicate, and ultramafic rocks, is considered to be correlative of the Maubisse Formation but passed through a distinct tectonic-metamorphic history [87,89].

The Banda Terrane, with Asian affinity, comprises: (1) the Lolotoi-Mutis Complex, with mica schist, graphitic phyllite, peridotite, and greenschist; (2) the Cretaceous turbidites of the Haulasi Formation; (3) the Late Paleocene-Middle Eocene thick-bedded limestones of the Dartollu Formation; (4) the Eocene to Oligocene Barique Formation that includes distinct volcanic suites and intercalated sedimentary rocks; (5) the Late Miocene to Pliocene Manamas Formation, the youngest volcanic unit of the Banda Terrane, composed of a km-thick pile of pillow basalt and tuffs.

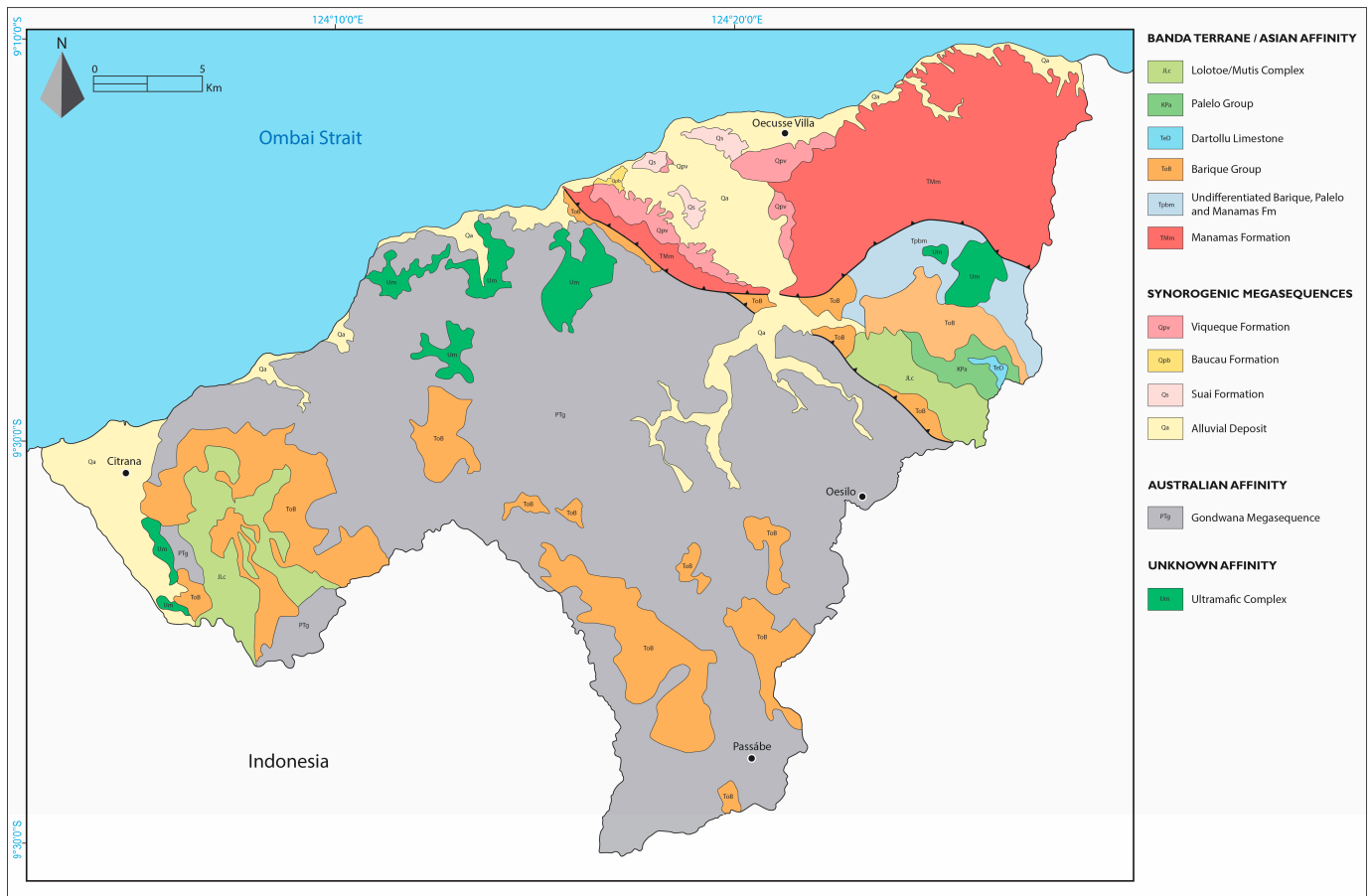


**Figure 2.** Geological sketch of Oecusse enclave with the catchment areas for the analyzed stream samples.

The Synorogenic Megasequence was deposited after and during the arc-continent collision. Its most voluminous units are (1) the Pliocene Viqueque Formation, mainly consisting of fossiliferous marls; (2) the Pliocene-Pleistocene Baucau coral reef limestones and conglomerate of Suai Formation; (3) recent alluvial and beach deposits.

Timor has a tropical hot climate, mainly influenced by the West Pacific Monsoon System. Seasonally, it displays a period with high rainfall intensity (wet season) and a period with low rainfall intensity (dry season). The wet season usually runs from December to May, and the dry season from June to November, although the wet season in the southern portions of the country lasts longer. Timor's annual rainfall varies across the country from north to south, normally being higher in higher altitude areas. It ranges from 1000 mm on the northern coast to 1500–2000 mm on the central part and more than 2500 mm on the area with high elevation located in the western part of the country [90].

### 3. Methodology

#### 3.1. Sampling

A sum of 82 stream sediment samples were obtained from streams of 1st and 2nd order. The sampling took place during the dry season, considering the elevated river flow patterns during the wet season in the study area. These patterns could lead to increased runoff rates and brief deposition periods, consequently leading to reduced concentrations of dissolved solids [91,92].

Sampling locations were identified using a global positioning system (GPS), and the sampling sites were chosen to be as uncontaminated as possible. Therefore, locations affected by pollution, such as near factories, heavy traffic roads, and arable soils, were avoided. Fresh samples were collected in plastic bags and transported to the laboratory for further analysis.

### 3.2. Chemical Analysis and Data Treatment

The <80 mesh fraction was properly weighed and sent to certified Activation Laboratories (Ancaster, ON, Canada) for chemical analysis and analyzed under the Ultratrace 3 package. The Chemical analyses were performed using INAA in the total sample and ICP-MS by total acid digestion (HNO<sub>3</sub>-HClO<sub>4</sub>-HF). Compared to other elements, Hg is particularly “troublesome” when analyzed by ICP-MS because it can easily evaporate and get trapped in the plastic tubing and glass parts of the sample introduction system. However, this was prevented by adding small amounts of HCl or Au to the diluent. Additionally, for quality control, the laboratory used the reference samples GXR4, GXR6, SDC-1, OREAS97, OREAS-45d, OREAS96, DNC-1a, SBC 1, and DMMAS 121. So, the results obtained in the analyses are accurate.

Following the verification of data normality and variance homogeneity, univariate and multivariate statistical analyses were conducted using JMP Pro 14.0 software. A Principal Component Analysis (PCA) based on a correlation matrix was performed to identify associations among the ten metal(loid) variables across the 82 sampling sites and to examine the relationship between the PTEs and the various geological units.

## 4. Results and Discussion

### 4.1. Univariate and Multivariate Statistics

Statistics of the analyzed metal(oid) concentrations from stream sediments were calculated and listed in Table 1 and Figure 3. Only total concentration was used; no valence state or heavy metal forms were included. Except for Hg, whose concentrations are low and frequently close to the detection level, all elements yield asymmetric distributions with a median smaller than the mean. Differences between mean and median are particularly high for Ni and, in particular, Cr, with one sample yielding more than 100 times the median value, and 9 samples are natural outliers with high Cr contents. The elements with the most variable concentrations are As and Cr (variance coefficient > 2; maximums almost three orders of greatness higher than minimum values). Among the elements with more homogenous concentrations, two are found at very low grades (Cd and Hg), two tend to be abundant in mafic rocks (Co and V), while others are common in felsic rocks or do not display a clear affinity with mafic or felsic material (U and Mn, Cu and Pb).

**Table 1.** Summary statistics for PTEs in stream sediments of littoral Oecusse.

mg/kg	As	Cd	Co	Cr	Cu	Hg	Mn	Ni	Pb	U	V	Zn
Minimum	0.25	0.05	14	28	19	0.005	823	11.2	0.9	0.1	36	52.2
Median	7.7	0.05	33.9	270.5	41.45	0.04	1580	64.3	11.35	1.1	84	87.1
Mean	10.79	0.085	36.7	1776.5	46.03	0.04	1660.8	154.7	12.23	1.01	111.8	94.1
maximum	214	0.4	142	25940	437	0.08	5140	1520.0	67.3	2.3	362	267
DP	23.74	0.071	18.4	3880.0	44.7	0.014	582.4	225.5	9.3	0.55	77.9	34.0

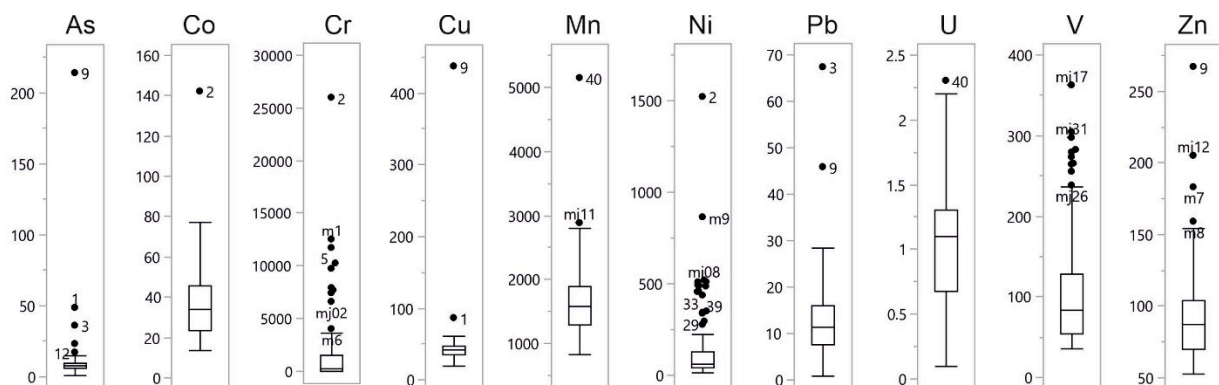


**Figure 3.** Boxplots of PTEs concentration in the studied sediments.

High concentrations of Cr and Ni are observed in a few stream sediments sourced by units of the Gondwana Megasequence (Maubisse Formation), its correlative metamorphic unit (Aileu Complex), the Banda Terrane (Barique and Manamas formations) or the Bobonaro mélange. The highest grades of Co, Cr, and Ni are observed in one sample with a drainage area occupied mainly by ultramafic rocks. Several sediments with drainage areas, mostly in the Lolotoi-Mutis Complex, yield high contents of As, Cu, Mn, Pb, and Zn, but the most elevated concentrations of Mn and U occur in sediments sourced by the Maubisse Formation. Vanadium is particularly abundant in stream sediments fed by the basaltic rocks of the Manamas Formation, along with sedimentary units derived from this volcanic succession, and in a few samples with catchment areas draining different volcanic and sedimentary units of the Gondwana Megasequence and Banda Terrane.

The principal component analysis (PCA) for the studied area stream sediments PTEs' data (Figure 4) allowed the determination of major associations among PTEs that can be ascribed to geological units. Using all samples and all PTEs as variables (Figure 4, above), the first 2 components of the PCA (PC1 and PC2; 61% of total variance) reveal strong associations Cr-Ni-Co and As-Cu. Cobalt, Cr, Ni, and V are plotted in opposition to U in the PC1 axis. The PCA is strongly affected by the extreme contents of As and Cu in a stream deposit sourced by metamorphic and basaltic rocks of the Banda Terrane (sample 9), and Cr, Ni, and Co in a small catchment draining almost exclusively ultramafic rocks (sample 2). A PCA without these samples (Figure 4, below) is more adequate to understand the relations between variables and possible links with drainage geology. The first two components provided by this PCA (65% of total variance) confirm the strong association Cr-Ni. In the PC1-PC2 biplot, As, Pb, and U appear together in opposition to V. Cobalt is plotted between Cr-Ni and V.

The basaltic rocks of Maubisse, Barique, and Manamas formations, which can be incorporated in the Bobonaro mélange, appear to be the most common sources of sediments with high Cr and Ni. The PC1-PC2 biplot suggests that a compositionally different set of igneous rocks belonging to the Maubisse, Barique, and Manamas formations and their covering sedimentary sequences are enriched in V. On the other end, sediments with high contents of As, Pb, and U appear to be preferentially linked to the metamorphic units of the Banda Terrane (Lolotoi-Mutis Complex). The Cu-Pb-As association may also indicate the impact of anthropogenic sources, such as the potential use of fertilizers or pesticides containing these elements and/or batteries, particularly in areas near population settlements [93], however due to the absence of significant urban centers close to the sampling points where these elements yield high grades of Cu, Pb and As the hypothesis of human sources for these elements appears unlikely.

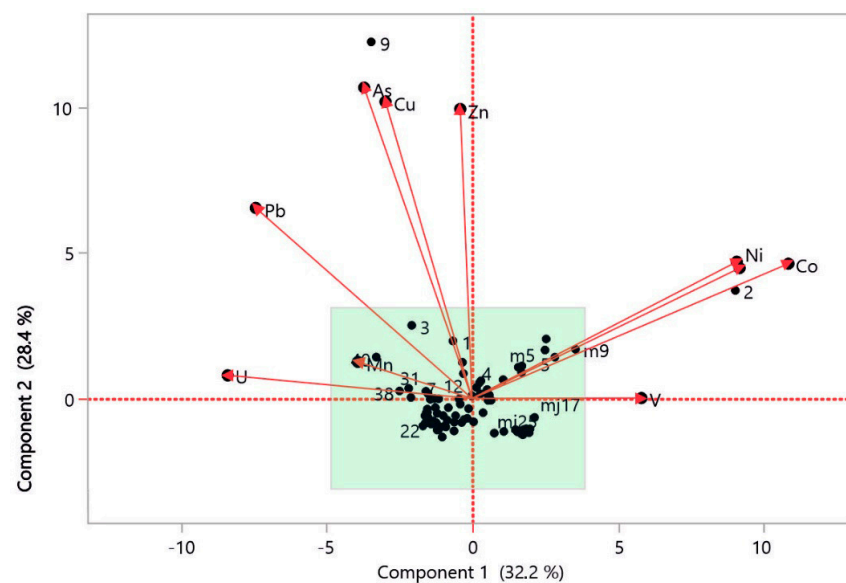
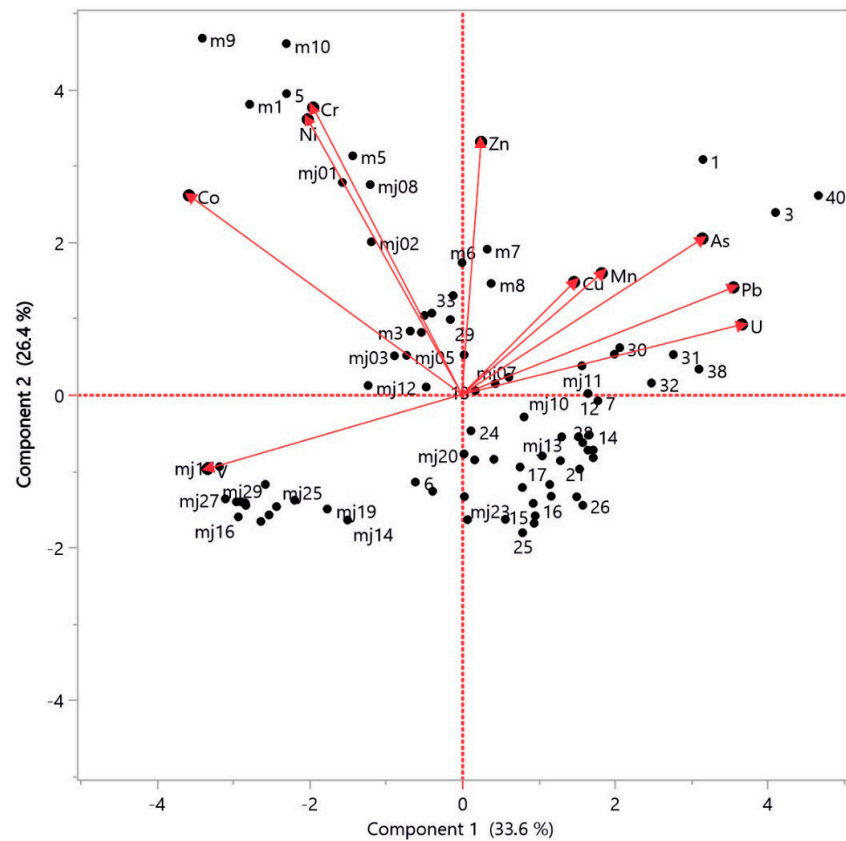


Figure 4. Cont.



**Figure 4.** Biplot with the representation of variables and samples in the two principal components (PC1 and PC2) obtained with PCAs performed with all samples (**above**) and without samples 9 and 2 (**below**).

4.2. Ecologic Risks

Because there are no legislated ecological guidelines for Timor Island, PTE contents in collected stream sediments were compared with guideline values that have been adopted by other countries. Table 2 shows that median values of PTEs of some stream sediments from Oecusse are higher than guideline limits adopted in Canada, Netherlands, South Africa, and Portugal for As, Co, Cr, Cu, and Ni. This is in accordance with the findings of Vicente et al. [69], which found anomalous or higher Cr, Ni, and Co than the expected contents.

**Table 2.** Median values obtained with the stream sediments of Oecusse for the analyzed hazardous elements ( $\text{mg kg}^{-1}$ ) and admissible levels according to the Canadian [94], Dutch [95], South African [96], and Portuguese [97] guidelines.

	Median	Canadian Guidelines	Dutch Guidelines	South Africa Guidelines	Portugal Guidelines
As	8	6	29	5.8 7.5	18
Cd	0.1	0.6	0.8	7.5	1.2
<b>Co</b>	33	50	9	18	21
<b>Cr</b>	324	26	100	46	69
Cu	42	16	36	16	92
Mn	1630	-	-	740	-
<b>Ni</b>	63	16	36	9.1	37
Pb	12	31	85	20	120
U	1.1	86	80	1.9	2.5
V	84	86	-	155	-
Zn	90	120	140	240	290

Note: Chemical elements in bold means that the its median concentrations are higher than the guidelines.

Numerous indices were used to assess the geochemical transformations promoted by contamination, either geogenic or anthropogenic. The Potential Ecological Risk Index (PERI) was used for the first time by Håkanson [98] to study sediment-related pollution and is being adopted by several authors [99–102]. It provides an indication of major contamination agents and the identification of sites where studies could prioritize. It is adopted to evaluate the level of contamination by multiple elements based on their potential toxic effects or environmental risks. This is defined as the cumulative sum of the risk factors associated with the contaminants in a sample, providing an assessment of contamination levels relative to their toxicity and environmental impact [103,104]. To normalize the PTEs for index calculations, Håkanson [98] recommends using values from the Upper Continental Crust. However, given that the study area includes outcropping units linked to the oceanic crust and potentially the upper mantle, we opted to normalize the PTEs using the median values for the entire area.

Table 3 shows the formulas of PERI, Pn, and Cfi and their respective explanation. For each potentially harmful element, Cfi was calculated using element concentration in the sample and regional median values. The single index of ecological risk factor (Pn) combines the element Cfi with the toxic response factor of individual metal Tn (which expresses the toxic response of individual metal(loid)s). PERI results from the sum of potential risks of individual metals Pn.

**Table 3.** Formulas of PERI, Pn, Cfi, and respective definitions.

Parameter	Explanation
$PERI = \sum P_n$	Pn: potential ecological risk factor of individual PTE. PERI < 95: low potential ecological risk; $95 \leq PERI < 190$ : moderate ecological risk; $190 \leq PERI < 380$ : considerable ecological risk and $PERI \geq 380$ : very high ecological risk.
$P_n = T_n \times C_{F_i}$	Tn (toxic response factor), which expresses the toxic response of individual metals. Tn for As, Cd, Co, Cr, Cu, Hg, Mn, Ni, V, Pb, and Zn are 30, 30, 2, 2, 5, 40, 10, 5, 1, 5, 1, respectively [101,105,106]. Pn classified as: $P_n < 40$ : low potential ecological risk; $40 \leq P_n < 80$ : reasonable ecological risk; $80 < P_n < 160$ : considerable ecological risk; $160 \leq P_n < 320$ : high ecological risk and $P_n \geq 320$ : very high ecological risk
$C_{F_i} = C_{\text{sample}} / \text{Median}$	C: element (i) concentration

The concentration of several elements in stream deposits constitutes high or very high potential ecological risks (Figure 5). Namely: for As in one sample sourced by the Lolotoi-Mutis Complex and basalts of the Barique Formation and one sample that results from sediment recycling of ultramafic rocks; for Cr and Ni grades in deposits partially fed by ultramafic rocks; for Co and Cu grades in the stream deposit sourced by the Lolotoi-Mutis Complex and basalts of the Barique Formation that also yield high As.

The index PERI is only very high in a stream sample sourced by the Lolotoi-Mutis Complex collected at the western Oecusse region (Figure 6). The grades of As, coupled with Co and Cu, account for this high PERI value. Considerable values of the PERI index were determined in 3 deposits, also from the western portion of Oecusse. Arsenic, Cr, and Ni are the elements with higher potential ecological risk factors in these deposits. Moderate values of PERI occur in wider areas of both center and western littoral Oecusse, also due to As, Cr, and Ni concentrations.



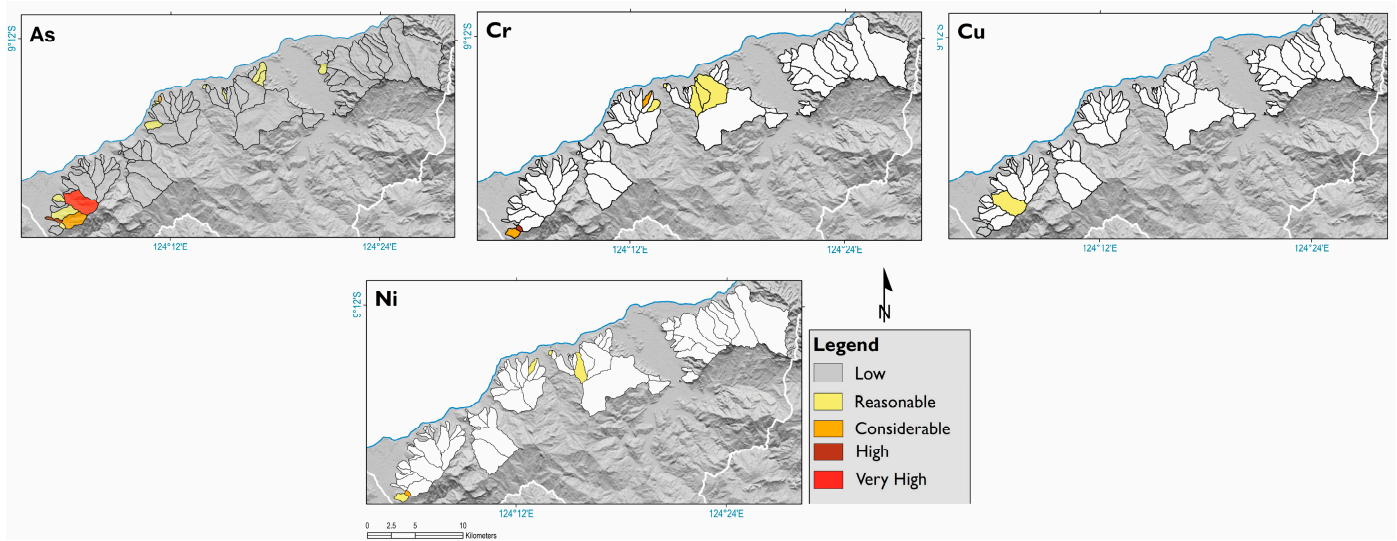


**Figure 5.** Potential ecological risk factors were determined for As, Cr, Cu, Ni, and V, elements that gave  $P_n > 40$ .

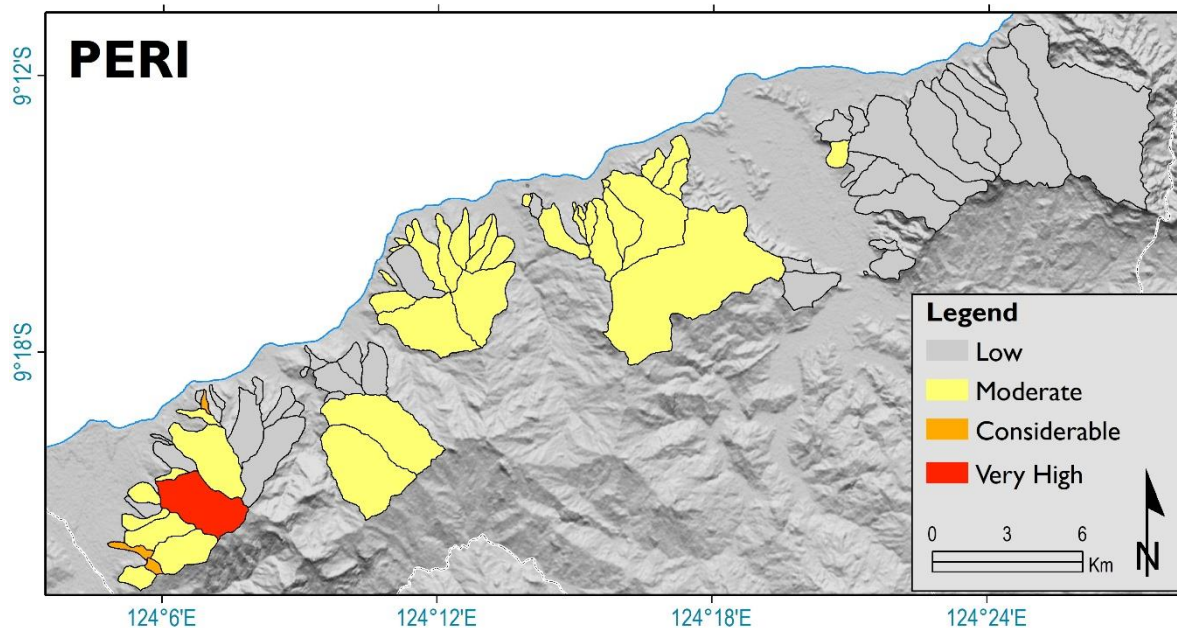


**Figure 6.** PERI values were determined with littoral sediments from Oecusse.

#### 4.3. Assessment of Health Risks Associated with Exposure PTEs

##### 4.3.1. Non-Carcinogenic Risk

The human health risk caused by trace elements exposure is expressed as hazard quotient ( $HQ = ADD/RfD$ ). The ADD is the average daily dose to which a child or adult is exposed, whereas RfD is the reference dose, which is the daily dosage that enables the exposed individual to sustain this level.

Noncancer risk can be evaluated with the hazard index (HI) for multiple substances and considering distinct exposure pathways [34]. The values of HI are obtained with the sum of the hazard quotient (HQ) for each element and each pathway. It is considered that there is a very low chance of noncarcinogenic risk where  $HI < 1$ . Exposure to potentially toxic elements (As, Cr, Pb, Cu, Ni, and Zn) through three pathways (i.e., ingestion, inhalation, and dermal contact) by two population sub-groups (adults and children) was calculated using equations described in USEPA [107,108]. Daily intake (CDI) was evaluated for exposure through ingestion ( $ADD_{ing}$ ), inhalation ( $ADD_{inh}$ ), and dermal contact

(ADD<sub>derm</sub>) by adopting values given in Table 4 and using the following Equations (1)–(3), where C<sub>s</sub> stands for the concentration of PTEs in stream sediments (mg kg<sup>-1</sup>):

$$ADD_{ing} = \frac{C_s \times IngR \times EF \times ED \times CF}{BW \times AT} \quad (1)$$

$$ADD_{inh} = \frac{C_s \times InhR \times ET \times EF \times ED}{PEF \times BW \times AT} \quad (2)$$

$$ADD_{derm} = \frac{C_s \times SA \times AF \times ABS \times EF \times ED \times CF}{BW \times AT} \quad (3)$$

**Table 4.** Values used in the determination of chronic daily intake (CDI) following the recommendation of USEPA [108].

Parameter	Unit	Adult Value	Children Value
IR	mg/day	100	200
EF	Days/Year	312	312
ED	Years	35	6
BW	Kg	70	15
ATnc	Days	375 × 35	365 × 6
ATc	Days	365 × 70	365 × 70
CF	mg/day	10 <sup>-6</sup>	10 <sup>-6</sup>
SA	cm <sup>2</sup>	6032	2373
AF	mg/cm <sup>2</sup>	0.07	0.2
ABS	Unitless	0.001	0.001
InhR	m <sup>3</sup> /h	1.56	1.2
ET	h/day	8	4
PEF	m <sup>3</sup> /day	1.36 × 10 <sup>9</sup>	1.36 × 10 <sup>9</sup>

Notes: IR: Ingestion rate; BW: Body weight; EF: Exposure frequency; ED: Exposure duration; ATc: Av. Time for carcinogenic risk; ATnc: AV. Time for noncarcinogenic risk; SA: Skin surface area available for contact; CF: Conversion factor; AF: Soil-to-skin adherence factor; ABS: Absorption factor; InhR: Inhalation rate; ET: Exposure time; PEF: Particulate emission factor.

The concentrations of various elements in the stream sediments under study may pose health risks to humans (Figure 7). The highest values of HI were determined with Cr, in particular for children, with HI being higher than 10 in 12 stream deposits sourced by ultramafic units and their covering sedimentary successions. High HI values for Cr are most common at the center-littoral portion of Oecusse. Where patches of the ultramafic rocks occur at the western portion of the territory, even if they only represent minor portions of the catchment areas, the Cr risk is still non-negligible. For adults, only the ultramafic rocks appear to supply Cr in sufficiently high concentrations to constitute health risks. However, the basalts of the Manamas Formation and, to a lesser extent, of Barique Formation can also be responsible for Cr exposure, compromising children's health.

Non-negligible risks were also obtained for exposure to As, Mn, and V. The most elevated values of HI for Mn were detected in sediments sourced by Maubisse and Barique formations. In the case of Barique, high values occur in sediments draining a rhyo-dacitic suite, which can also be present in the Maubisse Formation [109]. It is then reasonable to assume that these rocks are a likely source of Mn in the studied sediments. Regarding As, an HI > 1 was found only in a stream deposit from the western portion of Oecusse, whose catchment area drains in sub-equal proportions to the Lolotoi-Mutis Metamorphic Complex and basalts of the Barique Formation. Almost all sediments sourced by the Manamas Formation gave HI > 1 for V.

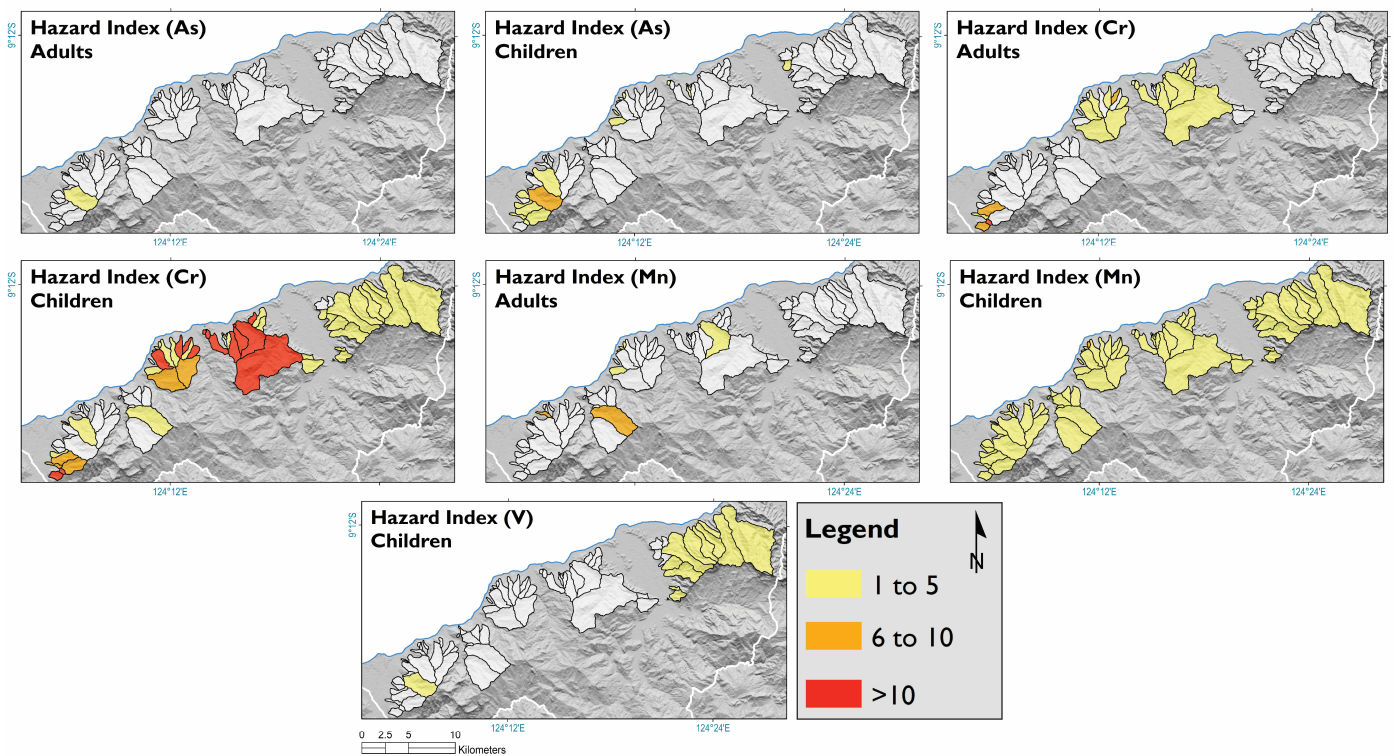


**Figure 7.** Non-carcinogenic hazard indexes associated with exposure to As, Cr, Mn, and V by different population groups. Only areas where chemical elements are higher than 1 ( $HI < 1$ ) are painted.

#### 4.3.2. Carcinogenic Risks

The carcinogenic risks for the population of the Oecusse enclave were assessed based on exposure to As, Cd, Cr, and Ni. These calculations were performed using Equation (4) from the Exposure Factors Handbook [110] and the slope factor (SF) values provided in [111].

$$\text{CancerRisk} = \sum (\text{ADD}_{\text{pathway}} \times \text{SF}_{\text{pathway}}) \quad (4)$$

The carcinogenic risks associated with As exposure via ingestion, inhalation, and dermal contact were evaluated using Equations (5)–(7):

$$\text{ILCR}_{\text{ing}} = \text{ADD}_{\text{ing}} \times \text{CSF}_{\text{ing}} \quad (5)$$

$$\text{ILCR}_{\text{inh}} = \text{ADD}_{\text{inh}} \times \text{CSF}_{\text{inh}} \quad (6)$$

$$\text{ILCR}_{\text{derm}} = \text{ADD}_{\text{derm}} \times \text{CSF}_{\text{derm}} \quad (7)$$

The  $\text{ILCR}_{\text{ing}}$ ,  $\text{ILCR}_{\text{inh}}$ , and  $\text{ILCR}_{\text{derm}}$  represent the incremental lifetime cancer risks for ingestion, inhalation, and dermal exposure pathways, respectively (dimensionless).

$\text{CSF}_{\text{ing}}$ ,  $\text{CSF}_{\text{inh}}$ , and  $\text{CSF}_{\text{derm}}$  are the cancer slope factors [110,111] through ingestion, inhalation, and dermal contact, respectively ( $[\text{mg}/\text{kg}\text{-day}]^{-1}$ ). The total incremental lifetime cancer risk (TILCR) was obtained by summing the ILCRs from all three exposure routes. A TILCR exceeding  $1 \times 10^{-6}$  is generally considered unacceptable and indicative of potential carcinogenic health effects for the exposed population, according to USEPA [110]. However, the concentrations found in stream sediments do not indicate a carcinogenic risk related to As exposure.

Chromium was the only element detected in stream sediments at concentrations high enough to increase cancer risk. Calculations were performed exclusively for inhalation exposure, as it is the only pathway with an available algorithm. Hazardous exposure poses a concern for both children and adults (Figure 8). Similar to non-carcinogenic risks, the

areas that demand the most attention are located in the central-littoral region of Oecusse, where ultramafic massifs are exposed.

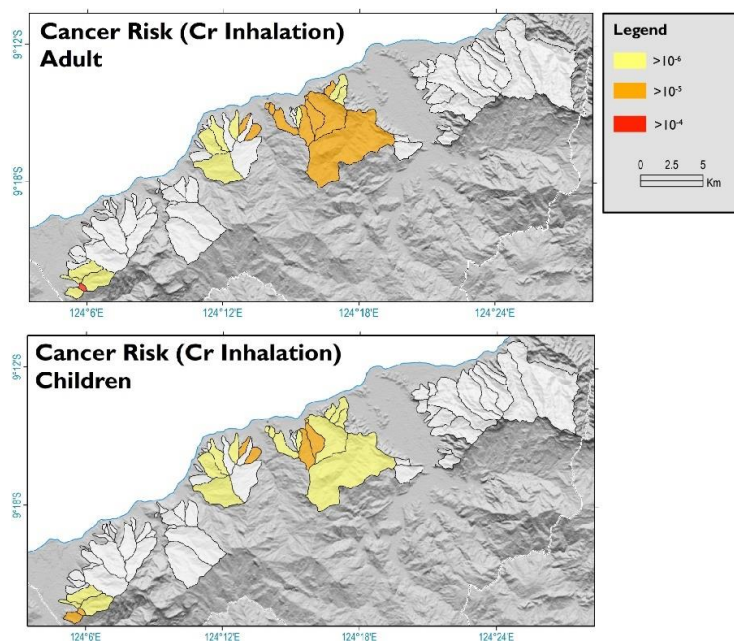


**Figure 8.** The carcinogenic risk associated with Cr. Only areas where Cr is higher  $10^{-6}$  which could imply CR are painted.

## 5. Conclusions

In-stream deposits from the coastal region of Oecusse, where outliers of ocean crust and upper mantle units crop out, the median concentrations of As, Co, Cr, Cu, and Ni exceed the allowable thresholds adopted in Canada, Netherlands, South Africa, and Portugal, reflecting the high natural concentration of these elements. The potential ecological risk factors reach high values for As, Cr, and Ni. The PERI is extremely high in a stream sample sourced by the allochthonous Lolotoi-Mutis Complex. Considering health hazard risks, Cr is the element that displays the highest HI, particularly for children, with HI being higher than 10 in 12 sediments entirely or partially derived from ultramafic units. Also, basalts of the Manamas Formation and, to a lesser extent, of the Barique Formation may account for relatively high Cr exposure, compromising children's health. Significant HI was also found for As in stream deposit draining the Lolotoi-Mutis Metamorphic Complex and basalts of Barique Formation, for Mn in sediments sourced by the Maubisse and Barique formations, and for V in sediments sourced by the Manamas Formation. Cancer risk was recognized for Cr, both for children and adults in the same regions of non-carcinogenic risk, where ultramafic massifs crop out.

The present research shows the extent to which natural processes may be responsible for extremely high concentrations of some PTEs and the diverse association between some geological units and specific elements. Given that the measured levels of potentially toxic elements (PTEs) in stream sediments indicate potential harm to both the environment and human health, it is imperative to alert relevant authorities. They need to regulate regional activities, such as the use of river deposits as raw materials, agricultural development, or water resource exploitation in stream valleys. These findings underscore the importance of geochemical surveys of stream deposits for informing future policy decisions, which is especially crucial in developing countries like East Timor.

**Author Contributions:** Conceptualization, V.A.S.V., M.C.P. and J.A.M.S.P.; Methodology, V.A.S.V., P.D. and J.A.M.S.P.; Software, V.A.S.V. and P.D.; Formal analysis, V.A.S.V., M.C.P. and P.D.; Investigation, V.A.S.V. and M.C.P.; Resources, V.A.S.V. and J.A.M.S.P.; Writing – original draft, V.A.S.V., M.C.P. and P.D.; Writing – review & editing, J.A.M.S.P.; Supervision, J.A.M.S.P.; Funding acquisition, V.A.S.V. All authors have read and agreed to the published version of the manuscript.

**Funding:** Field work and chemical analyses were supported by the Instituto de Geociências de Timor-Leste (IGTL, East Timor).

**Data Availability Statement:** The original contributions presented in the study are included in the article, further inquiries can be directed to the corresponding author/s.

**Acknowledgments:** The authors thank the three reviewers, which helped to improve the manuscript, and also the the Instituto de Geociências de Timor-Leste (IGTL, East Timor), which supported the field work and chemical analyses.

**Conflicts of Interest:** The authors declare no conflict of interest.

## References

1. Horton, R.; Beaglehole, R.; Bonita, R.; Raeburn, J.; McKee, M.; Wall, S. From public to planetary health: A manifesto. *Lancet* **2014**, *383*, 847. [[CrossRef](#)] [[PubMed](#)]
2. Lewis, S.L.; Maslin, M.A. Defining the anthropocene. *Nature* **2015**, *519*, 171–180. [[CrossRef](#)]
3. Steffen, W.; Richardson, K.; Rockström, J.; Cornell, S.E.; Fetzer, I.; Bennett, E.M.; Biggs, R.; Carpenter, S.R.; De Vries, W.; De Wit, C.A.; et al. Planetary boundaries: Guiding human development on a changing planet. *Science* **2015**, *347*, 1259855. [[CrossRef](#)] [[PubMed](#)]
4. Steffen, W.; Grinevald, J.; Crutzen, P.; McNeill, J. The Anthropocene: Conceptual and historical perspectives. *Philos. Trans. R. Soc. A Math. Phys. Eng. Sci.* **2011**, *369*, 842–867. [[CrossRef](#)]
5. Cabral-Pinto, M.M.; Inácio, M.; Neves, O.; Almeida, A.A.; Pinto, E.; Oliveiros, B.; Ferreira da Silva, E.A. Human health risk assessment due to agricultural activities and crop consumption in the surroundings of an industrial area. *Expo. Health* **2020**, *12*, 629–640. [[CrossRef](#)]
6. Salminen, R.; Chekushin, V.; Tenhola, M.; Bogatyrev, I.; Gregorauskiene, V.; Fedotova, E.; Gregorauskiene, V.; Kashulina, G.; Niskavaara, H.; Polischuok, A.; et al. *Geochemical Atlas of Eastern Barents Region*; Gulf Professional Publishing: Houston, TX, USA, 2005.
7. De Vivo, B.; Lima, A.; Bove, M.A.; Albanese, S.; Cicchella, D.; Sabatini, G.; Di Lella, L.A.; Protano, G.; Riccobono, F.; Frizzo, P.; et al. Environmental geochemical maps of Italy from the FOREGS database. *Geochem. Explor. Environ. Anal.* **2008**, *8*, 267–277. [[CrossRef](#)]
8. Lado, L.R.; Hengl, T.; Reuter, H.I. Heavy metals in European soils: A geostatistical analysis of the FOREGS Geochemical database. *Geoderma* **2008**, *148*, 189–199. [[CrossRef](#)]
9. BBravo, S.; García-Ordiales, E.; García-Navarro, F.J.; Amorós, J.; Pérez-De-Los-Reyes, C.; Jiménez-Ballesta, R.; Esbrí, J.M.; García-Noguero, E.M.; Higuera, P. Geochemical distribution of major and trace elements in agricultural soils of Castilla-La Mancha (central Spain): Finding criteria for baselines and delimiting regional anomalies. *Environ. Sci. Pollut. Res.* **2019**, *26*, 3100–3114. [[CrossRef](#)]
10. Cinelli, G.; Tollefsen, T.; Bossew, P.; Gruber, V.; Bogucarskis, K.; De Felice, L.; De Cort, M. Digital version of the European Atlas of natural radiation. *J. Environ. Radioact.* **2019**, *196*, 240–252. [[CrossRef](#)]
11. De Caritat, P.; Cooper, M. *A Continental-Scale Geochemical Atlas for Resource Exploration and Environmental Management: The National Geochemical Survey of Australia*; The Geological Society of London: London, UK, 2016.
12. Musgrove, M. The occurrence and distribution of strontium in US groundwater. *Appl. Geochem.* **2021**, *126*, 104867. [[CrossRef](#)]
13. Smith, D.B.; Wang, X.; Reeder, S.; Demetriades, A. The IUGS/IAGC task group on global geochemical baselines. *Earth Sci. Front.* **2012**, *19*, 1–6.
14. Wang, X.; Team, T.C.S. Reprint of “China geochemical baselines: Sampling methodology”. *J. Geochem. Explor.* **2015**, *154*, 17–31. [[CrossRef](#)]
15. Zuzolo, D.; Cicchella, D.; Demetriades, A.; Birke, M.; Albanese, S.; Dinelli, E.; Lima, A.; Valera, P.; De Vivo, B. Arsenic: Geochemical distribution and age-related health risk in Italy. *Environ. Res.* **2020**, *182*, 109076. [[CrossRef](#)] [[PubMed](#)]
16. Desenfant, F.; Petrovský, E.; Rochette, P. Magnetic signature of industrial pollution of stream sediments and correlation with heavy metals: Case study from South France. *Water Air Soil Pollut.* **2004**, *152*, 297–312. [[CrossRef](#)]
17. Garrett, R.G.; Reimann, C.; Smith, D.B.; Xie, X. From geochemical prospecting to international geochemical mapping: A historical overview. *Geochem. Explor. Environ. Anal.* **2008**, *8*, 205–217. [[CrossRef](#)]
18. Smith, D.B.; Smith, S.M.; Horton, J.D. History and evaluation of national-scale geochemical data sets for the United States. *Geosci. Front.* **2013**, *4*, 167–183. [[CrossRef](#)]
19. Komatina, M. *Medical Geology: Effects of Geological Environments on Human Health*; Elsevier: Amsterdam, The Netherlands, 2004.
20. Panaullah, G.M.; Alam, T.; Hossain, M.B.; Loepfert, R.H.; Lauren, J.G.; Meisner, C.A.; Ahmed, Z.U.; Duxbury, J.M. Arsenic toxicity to rice (*Oryza sativa* L.) in Bangladesh. *Plant Soil* **2009**, *317*, 31–39. [[CrossRef](#)]
21. Yao, W.; Hu, C.; Yang, X.; Shui, B. Spatial variations and potential risks of heavy metals in sediments of Yueqing Bay, China. *Mar. Pollut. Bull.* **2021**, *173*, 112983. [[CrossRef](#)]
22. International Agency for Research on Cancer. Chromium, nickel and welding. *IARC Monogr. Eval. Carcinog. Risks Hum.* **1990**, *49*, 1–648.

23. Klotz, K.; Weistenhöfer, W.; Neff, F.; Hartwig, A.; van Thriel, C.; Drexler, H. The health effects of aluminum exposure. *Dtsch. Ärzteblatt Int.* **2017**, *114*, 653. [[CrossRef](#)]
24. Khan, M.S.; Ikram, M.; Park, J.S.; Park, T.J.; Kim, M.O. Gut microbiota, its role in induction of Alzheimer's disease pathology, and possible therapeutic interventions: Special focus on anthocyanins. *Cells* **2020**, *9*, 853. [[CrossRef](#)] [[PubMed](#)]
25. Bonfiglio, R.; Scimeca, M.; Mauriello, A. Addressing environmental pollution and cancer: The imperative of the 2030 agenda. *Future Oncol.* **2023**, *19*, 2273–2276. [[CrossRef](#)] [[PubMed](#)]
26. Djouina, M.; Esquerre, N.; Desreumaux, P.; Vignal, C.; Body-Malapel, M. Toxicological consequences of experimental exposure to aluminum in human intestinal epithelial cells. *Food Chem. Toxicol.* **2016**, *91*, 108–116. [[CrossRef](#)] [[PubMed](#)]
27. Miah, M.R.; Ijomone, O.M.; Okoh, C.O.; Ijomone, O.K.; Akingbade, G.T.; Ke, T.; Krum, B.; Martins, A.d.C.; Akinyemi, A.; Aranoff, N.; et al. The effects of manganese overexposure on brain health. *Neurochem. Int.* **2020**, *135*, 104688. [[CrossRef](#)]
28. Schneider-Hassloff, H.; Straube, B.; Nuscheler, B.; Wemken, G.; Kircher, T. Adult attachment style modulates neural responses in a mentalizing task. *Neuroscience* **2015**, *303*, 462–473. [[CrossRef](#)]
29. Santamaria, A.B.; Cushing, C.A.; Antonini, J.M.; Finley, B.L.; Mowat, F.S. State-of-the-science review: Does manganese exposure during welding pose a neurological risk? *J. Toxicol. Environ. Health Part B* **2007**, *10*, 417–465. [[CrossRef](#)]
30. Flynn, M.R.; Susi, P. Neurological risks associated with manganese exposure from welding operations—A literature review. *Int. J. Hyg. Environ. Health* **2009**, *212*, 459–469. [[CrossRef](#)]
31. Lu, L.; Zhang, L.L.; Li, G.J.; Guo, W.; Liang, W.; Zheng, W. Alteration of serum concentrations of manganese, iron, ferritin, and transferrin receptor following exposure to welding fumes among career welders. *Neurotoxicology* **2005**, *26*, 257–265. [[CrossRef](#)]
32. de Oliveira, M.; Santinelli, F.B.; Lisboa-Filho, P.N.; Barbieri, F.A. The blood concentration of metallic nanoparticles is related to cognitive performance in people with multiple sclerosis: An exploratory analysis. *Biomedicines* **2023**, *11*, 1819. [[CrossRef](#)]
33. Chen, X.J.; Ma, J.J.; Yu, R.L.; Hu, G.R.; Yan, Y. Bioaccessibility of microplastic-associated heavy metals using an in vitro digestion model and its implications for human health risk assessment. *Environ. Sci. Pollut. Res.* **2022**, *29*, 76983–76991. [[CrossRef](#)]
34. Farzan, S.F.; Eunos, H.M.; Haque, S.E.; Sarwar, G.; Hasan, A.R.; Wu, F.; Islam, T.; Ahmed, A.; Shahriar, M.; Jasmine, F.; et al. Arsenic exposure from drinking water and endothelial dysfunction in Bangladeshi adolescents. *Environ. Res.* **2022**, *208*, 112697. [[CrossRef](#)]
35. DesMarias, T.L.; Costa, M. Mechanisms of chromium-induced toxicity. *Curr. Opin. Toxicol.* **2019**, *14*, 1–7. [[CrossRef](#)]
36. Shahane, S.P.; Kumar, A. Estimation of health risks due to copper-based nanoagrochemicals. *Environ. Sci. Pollut. Res.* **2022**, *29*, 25046–25059. [[CrossRef](#)]
37. Zhang, Y.Y.; Li, X.S.; Ren, K.D.; Peng, J.; Luo, X.J. Restoration of metal homeostasis: A potential strategy against neurodegenerative diseases. *Ageing Res. Rev.* **2023**, *87*, 101931. [[CrossRef](#)]
38. Gupta, N.; Yadav, K.K.; Kumar, V.; Cabral-Pinto, M.M.; Alam, M.; Kumar, S.; Prasad, S. Appraisal of contamination of heavy metals and health risk in agricultural soil of Jhansi city, India. *Environ. Toxicol. Pharmacol.* **2021**, *88*, 103740. [[CrossRef](#)]
39. Kumar, A.; Pinto, M.C.; Candeias, C.; Dinis, P.A. Baseline maps of potentially toxic elements in the soils of Garhwal Himalayas, India: Assessment of their eco-environmental and human health risks. *Land Degrad. Dev.* **2021**, *32*, 3856–3869. [[CrossRef](#)]
40. Pinto, M.M.S.C.; Marinho-Reis, A.P.; Almeida, A.; Freitas, S.; Simões, M.R.; Diniz, M.L.; Pinto, E.; Ramos, P.; da Silva, E.F.; Moreira, P.I. Fingernail trace element content in environmentally exposed individuals and its influence on their cognitive status in ageing. *Expo. Health* **2019**, *11*, 181–194. [[CrossRef](#)]
41. Kurniawan, I.A.; Abdurrachman, M.; Sakakibara, M.; Xiaoxu, K.; Meilano, I.; Basuki, N.I.; Sucipta, I.G.B.E.; Arifa, A.N. Mercury Exposure from Artisanal Small-Scale Gold Mining in Bunikasih, West Java, Indonesia. In *Selected Studies in Environmental Geosciences and Hydrogeosciences*; Springer Nature Switzerland: Cham, Switzerland, 2020; pp. 95–98.
42. Alodia, G.; Dyan, P.; Sobarudin, N.; Adrianto, D.; Dwinovantyo, A.; Solikin, S.; Hanafi, M.; Pamumpuni, A.; Kurniawan, I.A.; Poerbandono; et al. Discovery of a conical feature in Halmahera waters, Indonesia: Traces of a late-stage hydrothermal activity. *Geosci. Lett.* **2023**, *10*, 47. [[CrossRef](#)]
43. Cabral Pinto, M.M.; Marinho-Reis, A.P.; Almeida, A.; Ordens, C.M.; Silva, M.M.; Freitas, S.; Simões, M.R.; Moreira, P.I.; Dinis, P.A.; Diniz, M.L.; et al. Human predisposition to cognitive impairment and its relation with environmental exposure to potentially toxic elements. *Environ. Geochem. Health* **2018**, *40*, 1767–1784. [[CrossRef](#)]
44. Schroeder, H.A. Cadmium, chromium, and cardiovascular disease. *Circulation* **1967**, *35*, 570–582. [[CrossRef](#)]
45. Cabral Pinto, M.M.; Ordens, C.M.; Condesso de Melo, M.T.; Inácio, M.; Almeida, A.; Pinto, E.; Ferreira da Silva, E.A. An inter-disciplinary approach to evaluate human health risks due to long-term exposure to contaminated groundwater near a chemical complex. *Expo. Health* **2020**, *12*, 199–214. [[CrossRef](#)]
46. Handoko, A.D.; Sapiie, B.; Rudyawan, A. Geochemical and geological properties of tin related to ore deposits: A Review. *IOP Conf. Ser. Earth Environ. Sci.* **2023**, *1245*, 012023. [[CrossRef](#)]
47. Gerardo, B.; Nogueira, J.; Pinto, M.C.; Almeida, A.; Simões, M.R.; Freitas, S. Trace Elements and Cognitive Function in Adults and Older Adults: A Comprehensive Systematic Review. *Expo. Health* **2024**, 1–53. [[CrossRef](#)]
48. Ferré-Huguet, N.; Martí-Cid, R.; Schuhmacher, M.; Domingo, J.L. Risk assessment of metals from consuming vegetables, fruits and rice grown on soils irrigated with waters of the Ebro River in Catalonia, Spain. *Biol. Trace Elem. Res.* **2008**, *123*, 66–79. [[CrossRef](#)]
49. Cabral-Pinto, M.M.; Saha, N.; Ordens, C.M.; Pitta-Grós, D.; Carlos, G.; Dinis, P.; Marques, R.; Prudêncio, I.; Rocha, F.; Silva, E.A.F.d. Integrated Geochemical and Mineralogical Investigation of Soil from the Volcanic Fogo Island (Cape Verde): Implications for Ecological and Probabilistic Human Health Risks. *Expo. Health* **2023**, *15*, 1–17. [[CrossRef](#)]

50. Kolawole, T.O.; Ajibade, O.M.; Olajide-Kayode, J.O.; Fomba, K.W. Level, distribution, ecological, and human health risk assessment of heavy metals in soils and stream sediments around a used-automobile spare part market in Nigeria. *Environ. Geochem. Health* **2023**, *45*, 1573–1598. [[CrossRef](#)]
51. Mhungu, F.; Cheng, Y.; Zhou, Z.; Zhang, W.; Liu, Y. Estimation of the cumulative risks from dietary exposure to cadmium, arsenic, nickel, lead and chromium Guangzhou, China. *Food Chem. Toxicol.* **2023**, *178*, 113887. [[CrossRef](#)]
52. Xia, Y.; Wang, C.; Zhang, X.; Li, J.; Li, Z.; Zhu, J.; Zhou, Q.; Yang, J.; Chen, Q.; Meng, X. Combined effects of lead and manganese on locomotor activity and microbiota in zebrafish. *Ecotoxicol. Environ. Saf.* **2023**, *263*, 115260. [[CrossRef](#)]
53. Anderson, R.A. Trace elements and cardiovascular diseases. *Acta Pharmacol. Toxicol.* **1986**, *59*, 317–324. [[CrossRef](#)]
54. Tinkov, A.A.; Filippini, T.; Ajsuvakova, O.P.; Skalnaya, M.G.; Aaseth, J.; Bjørklund, G.; Gatiatulina, E.R.; Popova, E.V.; Nemereshina, O.N.; Huang, P.-T.; et al. Cadmium and atherosclerosis: A review of toxicological mechanisms and a meta-analysis of epidemiologic studies. *Environ. Res.* **2018**, *162*, 240–260. [[CrossRef](#)]
55. Satarug, S.; Vesey, D.A.; Gobe, G.C.; Phelps, K.R. Estimation of health risks associated with dietary cadmium exposure. *Arch. Toxicol.* **2023**, *97*, 329–358. [[CrossRef](#)]
56. Gupta, N.; Yadav, K.K.; Kumar, V.; Prasad, S.; Cabral-Pinto, M.M.; Jeon, B.H.; Kumar, S.; Abdellattif, M.H.; Alsukaibia, A.K. Investigation of heavy metal accumulation in vegetables and health risk to humans from their consumption. *Front. Environ. Sci.* **2022**, *10*, 791052. [[CrossRef](#)]
57. Sergi, C.M. Nickel's carcinogenicity: The need of more studies to progress. *Mil. Med. Res.* **2024**, *11*, 8. [[CrossRef](#)]
58. Lee, E.Y.; Flynn, M.R.; Lewis, M.M.; Mailman, R.B.; Huang, X. Welding-related brain and functional changes in welders with chronic and low-level exposure. *Neurotoxicology* **2018**, *64*, 50–59. [[CrossRef](#)]
59. Pesch, B.; Weiss, T.; Kendzia, B.; Henry, J.; Lehnert, M.; Lotz, A.; Berges, M.; Hahn, J.; Mattenklott, M.; Punkeenburg, E.; et al. Levels and predictors of airborne and internal exposure to manganese and iron among welders. *J. Expo. Sci. Environ. Epidemiol.* **2012**, *22*, 291–298. [[CrossRef](#)]
60. Flynn, M.R.; Susi, P. Manganese, iron, and total particulate exposures to welders. *J. Occup. Environ. Hyg.* **2009**, *7*, 115–126. [[CrossRef](#)]
61. Chen, P.; Bornhorst, J.; Aschner, M.A. Manganese metabolism in humans. *Front. Biosci.* **2018**, *23*, 1655–1679. [[CrossRef](#)]
62. Cabral Pinto, M.M.; Ferreira da Silva, E.A. Heavy Metals of Santiago Island (Cape Verde) alluvial deposits: Baseline value maps and human health risk assessment. *Int. J. Environ. Res. Public Health* **2019**, *16*, 2. [[CrossRef](#)]
63. Pinto, M.M.C.; Silva, M.M.; da Silva, E.A.F.; Dinis, P.A.; Rocha, F. Transfer processes of potentially toxic elements (PTE) from rocks to soils and the origin of PTE in soils: A case study on the island of Santiago (Cape Verde). *J. Geochem. Explor.* **2017**, *183*, 140–151. [[CrossRef](#)]
64. Kumar, A.; Kumar, M.; Pandey, R.; ZhiGuo, Y.; Cabral-Pinto, M. Forest soil nutrient stocks along altitudinal range of Uttarakhand Himalayas: An aid to Nature Based Climate Solutions. *Catena* **2021**, *207*, 105667. [[CrossRef](#)]
65. Grosbois, C.; Meybeck, M.; Lestel, L.; Lefèvre, I.; Moatar, F. Severe and contrasted polymetallic contamination patterns (1900–2009) in the Loire River sediments (France). *Sci. Total Environ.* **2012**, *435*, 290–305. [[CrossRef](#)]
66. McBride, M.B. Cadmium concentration limits in agricultural soils: Weaknesses in USEPA's risk assessment and the 503 rule. *Hum. Ecol. Risk Assess.* **2003**, *9*, 661. [[CrossRef](#)]
67. Mohammed, E.H.; Wang, G.; Xu, Z.; Liu, Z.; Wu, L. Physiological response of the intertidal copepod *Tigriopus japonicus* experimentally exposed to cadmium. *Aquac. Aquar. Conserv. Legis.* **2011**, *4*, 99–107.
68. Barletta, M.; Lima, A.R.; Costa, M.F. Distribution, sources and consequences of nutrients, persistent organic pollutants, metals and microplastics in South American estuaries. *Sci. Total Environ.* **2019**, *651*, 1199–1218. [[CrossRef](#)]
69. Vicente, V.A.; Pratas, J.A.; Santos, F.C.; Silva, M.M.; Favas, P.J.; Conde, L.E. Geochemical anomalies from a survey of stream sediments in the Maquelab area (Oecusse, Timor-Leste) and their bearing on the identification of mafic-ultramafic chromite rich complex. *Appl. Geochem.* **2021**, *126*, 104868. [[CrossRef](#)]
70. Rau, J.L. *Mineral–Hydrocarbon Database and Bibliography of the Geology of East Timor*; United Nations Development Programme: New York, NY, USA, 2002.
71. Fisher, R.; Ling, H.; Natonis, R.; Hobgen, S.; Kaho, N.R.; Mudita, W.; Markus, J.; Bunga, W.; Nampa, W. Artisanal and small-scale mining and rural livelihood diversification: The case of manganese extraction in West Timor, Indonesia. *Extr. Ind. Soc.* **2019**, *6*, 229–240. [[CrossRef](#)]
72. Sojka, M.; Ptak, M.; Jaskuła, J.; Krasniqi, V. Ecological and health risk assessments of heavy metals contained in sediments of Polish dam reservoirs. *Int. J. Environ. Res. Public Health* **2022**, *20*, 324. [[CrossRef](#)]
73. Purbonegoro, T.; Damar, A.; Riani, E.; Butet, N.A.; Cordova, M.R. Accumulation of Cd and Pb in sediments and Asian swamp eels (*Monopterus albus*) from downstream area of Cisadane River, Indonesia. *Environ. Monit. Assess.* **2024**, *196*, 496. [[CrossRef](#)]
74. Van Geen, A.; Zheng, Y.; Cheng, Z.; He, Y.; Dhar, R.K.; Garnier, J.M.; Rose, J.; Seddique, A.; Hoque, M.A.; Ahmed, K.M. Impact of irrigating rice paddies with groundwater containing arsenic in Bangladesh. *Sci. Total Environ.* **2006**, *367*, 769–777. [[CrossRef](#)]
75. Brammer, H.; Ravenscroft, P. Arsenic in groundwater: A threat to sustainable agriculture in South and South-east Asia. *Environ. Int.* **2009**, *35*, 647–654. [[CrossRef](#)]
76. Hu, B.; Li, G.; Li, J.; Bi, J.; Zhao, J.; Bu, R. Spatial distribution and ecotoxicological risk assessment of heavy metals in surface sediments of the southern Bohai Bay, China. *Environ. Sci. Pollut. Res.* **2013**, *20*, 4099–4110. [[CrossRef](#)]
77. Alasfar, R.H.; Isaifan, R.J. Aluminum environmental pollution: The silent killer. *Environ. Sci. Pollut. Res.* **2021**, *28*, 44587–44597. [[CrossRef](#)]

78. Shabbir, U.; Tyagi, A.; Elahi, F.; Aloo, S.O.; Oh, D.H. The potential role of polyphenols in oxidative stress and inflammation induced by gut microbiota in alzheimer's disease. *Antioxidants* **2021**, *10*, 1370. [CrossRef]
79. Mateo, D.; Marquès, M.; Torrente, M. Metals linked with the most prevalent primary neurodegenerative dementias in the elderly: A narrative review. *Environ. Res.* **2023**, *236*, 116722. [CrossRef]
80. Hellström, H.O.; Michaëlsson, K.; Mallmin, H.; Mjöberg, B. The aluminium content of bone, and mortality risk. *Age Ageing* **2008**, *37*, 217–220. [CrossRef]
81. Bonfiglio, R.; Sisto, R.; Casciardi, S.; Palumbo, V.; Scioli, M.P.; Palumbo, A.; Trivigno, D.; Giacobbi, E.; Servadei, F.; Melino, G.; et al. The impact of toxic metal bioaccumulation on colorectal cancer: Unravelling the unexplored connection. *Sci. Total Environ.* **2023**, *906*, 167667. [CrossRef]
82. Soares, A.T.G.; de Castro Silva, A.; Tinkov, A.A.; Khan, H.; Santamaría, A.; Skalnaya, M.G.; Skalny, A.V.; Tsatsakis, A.; Bowman, A.B.; Aschener, A.; et al. The impact of manganese on neurotransmitter systems. *J. Trace Elem. Med. Biol.* **2020**, *61*, 126554. [CrossRef]
83. Vrtička, P.; Bondolfi, G.; Sander, D.; Vuilleumier, P. The neural substrates of social emotion perception and regulation are modulated by adult attachment style. *Soc. Neurosci.* **2012**, *7*, 473–493. [CrossRef]
84. Chen, G.; Huang, N.; Wu, G.; Luo, L.; Wang, D.; Cheng, Q. Mineral prospectivity mapping based on wavelet neural network and Monte Carlo simulations in the Nanling W-Sn metallogenic province. *Ore Geol. Rev.* **2022**, *143*, 104765. [CrossRef]
85. Ishaq, M.; Khalid, J.; Qaiser, Z.; Sarfraz, W.; Ejaz, U.; Naeem, N.; Masood, A.; Tufail, A.; Arshad, K.; Zaka, S.; et al. Nickel contamination, toxicity, tolerance, and remediation approaches in terrestrial biota. In *Bio-Organic Amendments for Heavy Metal Remediation*; Elsevier: Amsterdam, The Netherlands, 2024; pp. 479–497.
86. Hossini, H.; Shafie, B.; Niri, A.D.; Nazari, M.; Esfahlan, A.J.; Ahmadpour, M.; Nazmara, Z.; Ahmadimanesh, M.; Makhdoumi, P.; Mirzaei, N.; et al. A comprehensive review on human health effects of chromium: Insights on induced toxicity. *Environ. Sci. Pollut. Res.* **2022**, *29*, 70686–70705. [CrossRef]
87. Audley-Charles, M.G. Ocean trench blocked and obliterated by Banda forearc collision with Australian proximal continental slope. *Tectonophysics* **2004**, *389*, 65–79. [CrossRef]
88. Barber, A.J.; Audley-Charles, M.G.; Carter, D.J. Thrust tectonics in Timor. *J. Geol. Soc. Aust.* **1977**, *24*, 51–62. [CrossRef]
89. Charlton, T.R.; Barber, A.J.; Barkham, S.T. The structural evolution of the Timor collision complex, eastern Indonesia. *J. Struct. Geol.* **1991**, *13*, 489–500. [CrossRef]
90. Wallis, J. Victors, Villains, and Victims: Capitalizing on Memory in Timor-Leste. *Ethnopolitics* **2012**, *12*, 133–160. [CrossRef]
91. Fletcher, T.D.; Vietz, G.; Walsh, C.J. Protection of stream ecosystems from urban stormwater runoff: The multiple benefits of an ecohydrological approach. *Prog. Phys. Geogr.* **2014**, *38*, 543–555. [CrossRef]
92. Davis, A.P.; Traver, R.G.; Hunt, W.F.; Lee, R.; Brown, R.; Olszewski, J. Hydrologic performance of bioretention storm-water control measures. *J. Hydrol. Eng.* **2012**, *17*, 604–614. [CrossRef]
93. Dong, W.Q.Y.; Cui, Y.; Liu, X. Instances of soil and crop heavy metal contamination in China. *Soil Sediment Contam.* **2001**, *10*, 497–510. [CrossRef]
94. Canadian Legislation: Ministry of the Environment. *Soil, Ground Water and Sediment Standards for Use Under Part XV.1 of the Environmental Protection Act*; Canadian Legislation/Ministry of the Environment: Toronto, ON, Canada, 2011.
95. Ministry of Housing, Spatial Planning and the Environment (VROM). Circular on Target Values and Intervention Values for Soil Remediation. The Netherlands Government Gazette, No. 39, Ministry of Housing, Spatial Planning and Environment, Directorate General for Environmental Protection, Department of Soil Protection. Available online: [http://www.esdat.net/Environmental%20Standards/Dutch/annexS\\_I2000Dutch%20Environmental%20Standards.pdf](http://www.esdat.net/Environmental%20Standards/Dutch/annexS_I2000Dutch%20Environmental%20Standards.pdf) (accessed on 3 March 2021).
96. Environmental Affairs Republic of South Africa, DEA. *Framework for the Management of Contaminated Land of South Africa*; Environmental Affairs Republic of South Africa, DEA: Pretoria, South Africa, 2010.
97. Portuguese Agency for Environment (APA). *Amadora, Lisbon, January of 2019 (Revision 3—September 2022)*; Portuguese Agency for Environment (APA): Amadora, Portugal, 2019.
98. Håkanson, L. An ecological risk index for aquatic pollution control. *A Sedimentol. Approach. Water Res.* **1980**, *14*, 975–1001.
99. Ding, X.; Ye, S.; Yuan, H.; Krauss, K.W. Spatial distribution and ecological risk assessment of heavy metals in coastal surface sediments in the Hebei Province offshore area, Bohai Sea, China. *Mar. Pollut. Bull.* **2018**, *131*, 655–661. [CrossRef]
100. Islam, S.; Ahmed, K.; Al-Mamun, H. Distribution of trace elements in different soils and risk assessment: A case study for the urbanized area in Bangladesh. *J. Geochem. Explor.* **2015**, *158*, 212–222. [CrossRef]
101. Moni, F.N.; Miazi, M.S.A.; Kabir, M.H.; Shammi, R.S.; Islam, M.S.; Islam, M.S.; Sarke, M.; Khan, M.; Ahammed, S.; Siddique, A.; et al. Enrichment, sources, and distributions of toxic elements in the farming land's topsoil near a heavily industrialized area of central Bangladesh, and associated risks assessment. *Heliyon* **2023**, *9*. [CrossRef] [PubMed]
102. Diniz, L.; Carlos, G.; Miranda, C.; Dinis, P.; Marques, R.; Rocha, F.T.; da Silva, E.F.; Almeida, A.; Pinto, M.C. Soil Geochemical Mapping of the Sal Island (Cape Verde): Ecological and Human Health Risk Assessment. *Land* **2024**, *13*, 1139. [CrossRef]
103. Wu, J.; Lu, J.; Li, L.; Min, X.; Luo, Y. Pollution, ecological-health risks, and sources of heavy metals in soil of the northeastern Qinghai-Tibet Plateau. *Chemosphere* **2018**, *201*, 234–242. [CrossRef] [PubMed]
104. Maanan, M.; Saddik, M.; Maanan, M.; Chaibi, M.; Assobhei, O.; Zourarah, B. Environmental and ecological risk assessment of heavy metals in sediments of Nador lagoon, Morocco. *Ecol. Indic.* **2015**, *48*, 616–626. [CrossRef]
105. Kumar, A.; Suryadevara, N.; Hill, T.M.; Bezbradica, J.S.; Van Kaer, L.; Joyce, S. Natural killer T cells: An ecological evolutionary developmental biology perspective. *Front. Immunol.* **2017**, *8*, 1858. [CrossRef]



106. Doležalová Weissmannová, H.; Mihočová, S.; Chovanec, P.; Pavlovský, J. Potential ecological risk and human health risk assessment of heavy metal pollution in industrial affected soils by coal mining and metallurgy in Ostrava, Czech Republic. *Int. J. Environ. Res. Public Health* **2019**, *16*, 4495. [[CrossRef](#)]
107. USEPA (United States Environmental Protection Agency). *Risk Assessment Guidance for Superfund: Volume III—Part A, Process for Conducting Probabilistic Risk Assessment*; [EPA 540-R-02-002]; US Environmental Protection Agency: Washington, DC, USA, 2001.
108. USEPA (United States Environmental Protection Agency); Science Policy Council. *Guidance on Cumulative Risk Assessment. Part 1*; US Environmental Protection Agency: Washington, DC, USA, 2001.
109. USEPA (United States Environmental Protection Agency). *Guidelines for Exposure Assessment, Risk Assessment Forum*; [EPA/600/Z-92/001]; United States Environmental Protection Agency: Washington, DC, USA, 1992.
110. USEPA (United States Environmental Protection Agency). *Toxicological Review of Inorganic Arsenic*; U.S. Environmental Protection Agency: Washington, DC, USA, 2010.
111. Rim, K.T. Evaluations of carcinogens from comparison of cancer slope factors: Meta-analysis and systemic literature reviews. *Mol. Cell. Toxicol.* **2023**, *19*, 635–656. [[CrossRef](#)]

**Disclaimer/Publisher’s Note:** The statements, opinions and data contained in all publications are solely those of the individual author(s) and contributor(s) and not of MDPI and/or the editor(s). MDPI and/or the editor(s) disclaim responsibility for any injury to people or property resulting from any ideas, methods, instructions or products referred to in the content.